Polymer Testing 32 (2013) 665–672

Contents lists available at SciVerse ScienceDirect

Polymer Testing

journal homepage: www.elsevier.com/locate/polytest

Material properties

Polyurethane foams based on modified tung oil and reinforced with rice husk ash II: Mechanical characterization

Virginia Ribeiro da Silva [a,b,c], Mirna A. Mosiewicki [c], Maria Irene Yoshida [a], Mercês Coelho da Silva [d], Pablo M. Stefani [c], Norma E. Marcovich [c,*]

[a] Universidade Federal de Minas Gerais, Belo Horizonte, MG 31270-901, Brazil
[b] CAPES Foundation, Ministry of Education of Brazil, Brasília, DF 70040-020, Brazil
[c] Institute of Materials Science and Technology (INTEMA), University of Mar del Plata, National Research Council (CONICET), Juan B. Justo 4302, Mar del Plata 7600, Argentina
[d] Universidade Federal de Itajubá, Campus Itabira, Itabira, MG 35900-373, Brazil

ARTICLE INFO

Article history:
Received 24 January 2013
Accepted 6 March 2013

Keywords:
Polyurethane foam
Tung oil
Mechanical properties

ABSTRACT

Viscoelastic polyurethane (PU) foams based on modified tung oil, ethylene glycol and polymeric MDI, and reinforced with rice husk ash (RHA), were prepared by a free-rise pouring method and characterized in terms of density, compression and dynamic mechanical behavior. The density of foams ranged between 50 and 90 kg/m^3, depending on the position of the sample with respect to the foam rise direction and filler content. As revealed by dynamic mechanical tests, the foams exhibited two different and broad thermal transitions, the temperature of their maxima depending on filler concentration. Compression modulus, compressive strength and storage modulus increase as foam density increases but decreases as rice husk ash concentration increases due to the detrimental changes induced by the filler in the foam cellular structure. However, densification strain exhibits the opposite behavior, indicating that reinforced foams can sustain slightly higher deformations without collapsing, probably due to a reduced reactivity of the components induced by the filler.

1. Introduction

Polyurethane foam materials are widely used in applications such as packaging and cushioning, and are attracting increasing attention from engineers and researchers. They are basically made of interconnected networks of solid struts and cell walls interspersed by voids or pockets with entrapped gas. The attributes of high porosity, lightweight, high crushability and good deformation energy absorption are common to all foam materials. The conventional approach to describe the interconnected structure is to employ the term “cell” to represent the smallest structural unit. Cells are polyhedral in foams and their edges and faces are defined by struts and walls. The cell geometry (e.g. shape and size) and the way the cells are packed govern the microscopic distribution of the solid material within the cellular structure. Polyurethane (PU) foam manufactured by mixing liquid constituents and allowing them to react and expand (rise) upwards exhibits normal anisotropy: cells are generally elongated in the foam rise direction due to the foaming process, and this gives rise to mechanical anisotropy [1]. The final properties of reinforced cellular solids depend also on type and loading of fibers or particles and fiber length or particle diameter [2]. According to de Mello and co-workers [3], particle surface state, dispersion and filler amount are other critical parameters to define foam architecture and mechanical properties.

* Corresponding author. Tel.: +54 223 481 6600; fax: +54 223 481 0046.
E-mail address: marcovic@fi.mdp.edu.ar (N.E. Marcovich).

0142-9418/$ – see front matter © 2013 Elsevier Ltd. All rights reserved.
http://dx.doi.org/10.1016/j.polymertesting.2013.03.010

Due to the large amounts used, disposal of these foams causes concerns about their negative impact on the environment. Although a small portion of used plastic foam has been successfully recycled, most of the foams are disposed of in landfills. However, tougher environmental laws and increasing disposal costs have forced research institutions and industries to look for alternatives. Numerous attempts have been made to develop biodegradable materials to replace petrochemical-based loose-fill packaging materials [4]: Soyol (polyol derived from soy oil) based polyurethane foams, free from volatile organic compound, formaldehyde and asbestos, have been formulated to increase the renewable content in the end products. Tan et al. [5] studied how soy polyols affected foam properties by partially or completely replacing the petroleum-based polyol with a soybean oil-based polyol in a standard formulation suitable for appliance insulation. Gu et al. [6] reported the preparation and characterization of a soy-based PU foam formulated with maple pulp fiber, which could be fast foamed for insulation. Lee et al. [7] indicated that by reinforcing soybean oil derived polymer foams with bacterial cellulose nanofibers, a new type of green macroporous polymer nanocomposite could be manufactured *via* simple mechanical frothing of monomer. Mosiewicki et al. [8] synthesized and characterized a polyol obtained from castor oil and used it in the production of wood flour filled rigid polyurethane foams. Wang et al. [9] converted castor oil into its maleic acid ester and free-radically copolymerized it with styrene to obtain biodegradable plastic foams with high content of castor oil. Coll Ferrer et al. [10] reported the influence of synthetic and vegetable based polyols (oxypropylated derivatives of glycerol) on the final mechanical properties of polyurethane based networks. Wu et al. [11] prepared and characterized biofoam composites using short sisal fibers as reinforcement and acrylated epoxidized soybean oil as matrix, aiming at replacing traditional unsaturated polyester foams in structural applications. Casado et al. [12] obtained a biobased polyol by chemical modification of tung oil and used it in the production of compact polyurethane composites reinforced with pine wood flour. In a previous publication [13], we indicated that PU foams based on modified tung oil presented adequate physical-chemical properties to be considered as an alternative to replace petrochemical based materials. However, the mechanical performance of the foams is also important when semi-structural or construction applications are considered. Therefore, the aim of this work is to report the mechanical and dynamic mechanical behavior of green viscoelastic PU foams based on modified tung oil and polymeric MDI and reinforced with rice husk ash.

2. Experimental

2.1. Materials

The natural polyol was obtained from tung oil supplied by Cooperativa Agrícola Limitada de Picada Libertad, Argentina (saponification value = 223 mg KOH/g, acid number = 2.11 mg KOH/g). It was chemically modified in a two-step procedure to produce a final product which is a mixture of different alcohols containing one or two hydroxylated fatty acid chains with high viscosity (at room temperature) and an average hydroxyl number of 450 mg KOH/g, as reported in a previous publication [13]. Ethylene glycol (Sigma) was also used as a reactive diol, with the aim of reducing the viscosity of the polyol counterpart. The selected isocyanate was 4,4′-diphenylmethane diisocyanate (pMDI) prepolymer (Rubinate 5005, Huntsman Polyurethanes, USA) with an equivalent weight of 131 g/eq. The surfactant agent was a commercial silicone oil (Tergostab B8404® Huntsman Polyurethanes), the catalyst a tertiary amine (n,n-dimethyl benzyl amine - DMBA, Aldrich) and the foaming agent used was distilled water.

The rice husk (RH) used in the present work was collected from rice industries of Concepción del Uruguay (Entre Ríos, Argentina). Rice husk ash (RHA) was obtained by combustion of RH in air, using a laboratory oven that was heated from room temperature to 600 °C, at a rate of 10 °C min^{-1}. The sample was maintained at 600 °C for 90 min and then allowed to cool to room temperature inside the oven [14]. The obtained ash was further crushed using an analytic mill (IKA 50, Germany), for 10 min and only ash particles with size lower than 100 mesh (U.S. Standard, <150 μm) were used.

All the reagents were dried at 70 °C until constant weight in a vacuum oven before use in order to eliminate absorbed moisture.

2.2. Polyurethane foams synthesis

As in our previous publication [13] polyurethane foams were prepared using a polyol mass ratio = 9:1 (polyol from tung oil: ethylene glycol). The polyol blend, amine catalyst (1 wt.% with respect to the polyol blend content), surfactant agent (2.5 wt.% with respect to the polyol blend content) and distilled water (4 wt.% with respect to the polyol blend content) were mechanically stirred for 60 s to ensure complete mixing. After that, the pMDI was added in a equivalent NCO/OH ratio = 1.1 (the contributions of both polyols and water were considered in the OH calculation), the system was again mechanically stirred for 10 s and then allowed to freely rise in a 10 cm diameter beaker at room temperature. Neat and filled foams, containing up to 5 wt.% RHA, were obtained. In the case of rice husk ash reinforced foams, the inorganic material was added before the MDI.

2.3. Foam characterization

Density measurements: the density of the foams was obtained as the ratio between the weight and volume of a cylindrical specimen. The weight was measured with a precision of ±0.001 g and the sample linear dimensions (26 mm diameter and ~30 mm height) with ±0.01 mm. At least five replicated specimens of each sample were measured.

Scanning Electron Microscopy (SEM): was used to obtain photographs of unreinforced and ash reinforced foams. Small specimens were cut from the foam samples (middle height) using a thin blade and then immersed in liquid nitrogen to obtain cryo-fractured (fragile) surfaces. Samples were sputter-coated with gold prior to SEM

observation. A scanning electron microscope Philips model SEM 505 operated at 15 kV was used.

Compression tests: cylindrical specimens of 26 mm diameter × ~30 mm height were cut from the foams, and tested at room temperature in an INSTRON 8501 Universal testing machine, according to the ASTM D1621. The compression force was applied in the foam rise direction. Each foam was divided into two parts (in height) and at least four specimens of each part were tested. Samples were first compressed to 80% of the original length at a crosshead speed of 10 mm/min. The average values of compression modulus (calculated as the slope of the stress-strain curve at low deformations), compressive strength (in accordance with ASTM D1621, it was taken as the stress reached at the compressive yield point, since it occurs for all samples before 10% deformation) and densification strain (taken as the strain at the point of intersection between the horizontal plateau stress line and the backward extended densification line, as indicated by Tondi et al. [15]) were calculated from these tests.

Then, the samples were unloaded and allowed to recover for 1 min. The length reached after the recovery time (l_r) was compared to the initial specimen height (l_i) and used to calculate the recovery (R_r) ratio, as indicated in Equation (1):

$$R_r = \frac{l_i - l_r}{l_i} \times 100 \quad (1)$$

Finally, specimens were subjected to another compression test at the same crosshead speed and the compression modulus in this "deformed" condition was also evaluated.

Dynamic mechanical tests: the dynamic mechanical properties of the samples were determined using an Anton Paar, Physica MCR rheometer. Torsion geometry was used with solid rectangular samples of length = 30 mm, width = 10 mm and thickness = 3 mm. Measurements were performed as temperature sweeps in the range -50–130 °C at a heating rate of 10 °C/min. The frequency was kept in 1 Hz, and applied deformation at 0.1%, to ensure working in the linear viscoelastic range. The thermal transition temperatures were arbitrarily selected as the temperature of the maximum in the loss modulus curves.

3. Results and discussion

The foams were prepared using a mixture of a short diol (ethylene glycol) added to the high-functional polyol derived from tung oil, to reduce the viscosity of the initial (unreacted) system and, therefore, to allow good dispersion of the filler [13]. The addition of even relatively small amounts of rice husk ash to the liquid mixture led to a significant increase in the viscosity and creaming time, resulting in a less expandable mixture as the filler concentration increases [13]. This is a quite typical effect in the processing of reinforced polyurethane foams, as was reported elsewhere [6,16]. For this particular system it was corroborated that dispersing more than 5 wt.% RHA into the liquid reactive mixture was very difficult due to the high viscosity of the system. Moreover, the resulting foams presented undesirable properties [13]. Accordingly, the following discussion deals with samples containing up to 5 wt.% RHA.

Fig. 1 shows the scanning electron micrographs corresponding to the unfilled and 5 wt.% filled foams, analyzed in the transverse direction (sample A) or in the foam rise direction (sample B). Microscopic examination of the resulting internal structure reveals that both samples contain open and closed cells, the latter accounting for the greater portion in the unfilled sample [13]. The pictures corresponding to the unfilled foam indicated that these specimens have cells with quite similar shapes and sizes, these forms being almost independent of the direction of testing. On the contrary, the reinforced foam exhibits anisotropic geometry: cells are more elongated in the foam rise direction and also their shape and size distribution is wider than in the unreinforced samples. In particular, some cells with noticeably decreased size can be seen in the filled sample, which could indicate that the dispersed RHA particles acted as nucleating sites for cell formation, as was reported in related papers [13,17,18].

The effect of both the foam density and the filler concentration on the mechanical properties was investigated. To do this, specimens for compression tests were cut from the top or the bottom of the prepared free-rise foams and the measured densities are reported in Table 1. Clearly, the density of the specimens obtained form the bottom of the foams are higher than the corresponding samples cut from the top, in all cases. As was reported in related publications [3], density is related to foam contraction after the liberation of gases. At some point during foam development, the foam stops expanding, releases gases and contracts, accumulating mass at the bottom of the block. In addition, the overall trend of the foam density is to decrease as the concentration of RHA increases, which is attributed to the opposing effects of particle addition on nucleation and cell growth: the ash particles act as nucleation sites promoting the formation of a higher quantity of bubbles, and this tends to increase with the filler content. At the same time, growth of the resulting cells seems to be hindered by the increase in viscosity, as was also noted by other researchers [19,20]. In our case, the cells are allowed to expand more easily in the foams containing less than 5 wt.% than in those with higher concentrations and, therefore, a reduction of the final foam density is observed [13]. Moreover, the density of reinforced foams is a function of void fraction and filler content [14,21]. As the ash has higher density than neat polyurethane matrix, its incorporation should cause a density increase in the final foams. Hence, the results presented in Table 1 indicate clearly that the increase in density due to the incorporation of RHA is more than compensated by an increase in the void fraction [13] in all cases (i.e. samples cut from the top or the bottom of the free-rise foams).

Fig. 2 shows the compression stress-strain curves for selected specimens. As is the case of most rigid foams, the compressive stress-strain curves show a linear elastic region, followed by a stress-plateau region [15,22,23]. At the end of the latter, the stress starts increasing again. Obviously, the slope of the initial, linear, part of the curve is the Young's modulus; the stress reaches a peak value at the end of the elastic region that corresponds to the compressive

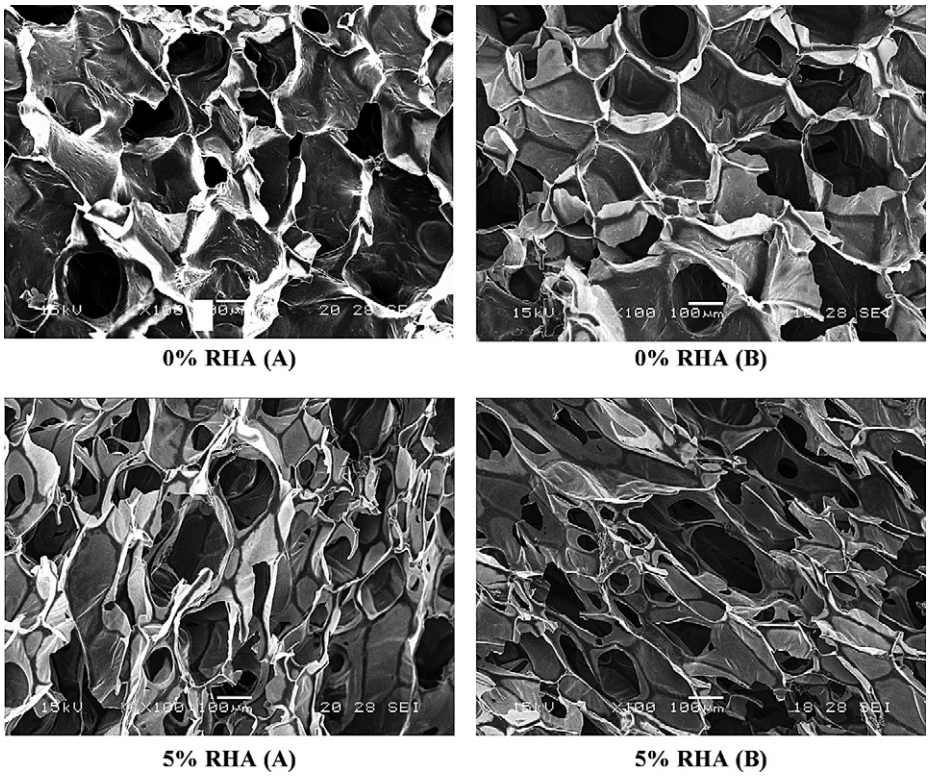

Fig. 1. Scanning electron micrographs corresponding to the unfilled and 5 wt.% filled foams, analyzed in the transverse direction (A) and in the foam rise direction (B).

strength. This maximum stress is sometimes followed by a decrease before the stress-plateau is reached [15,23], as exemplified in the curve corresponding to the 1 wt% filled sample taken from the bottom of the beaker. Cracks initiate at the peak stress value and the material tends to generate fragments as a result of these cracks. The long plateau, typically ranging from 6% to 50% strain for samples taken from the upper part of the foam, originates from the coexistence of collapsed and uncollapsed zones, typical of brittle foam undergoing successive cell wall fractures. Beyond the plateau, densification takes place and the stress rises sharply as complete densification begins. When total cell collapse is completed, the compacted material begins to behave like a homogenous solid [1]. From the curves presented in Fig. 2 it is clearly seen that stress value at the plateau decreases as filler concentration increases (except for 1 wt.% RHA, that behaves like the neat foam) and increases with foam density (i.e. increased from top to bottom of the foam block). As the absorbed energy during compression tests can be calculated as the area under the stress-strain curve, it is clear that the foams' capacity for compression energy dissipation decreases slightly as the filler concentration increases. Some published studies [24,25] showed that macro-particles disturb the macroscopic cell arrangement and decrease stiffness and compression resistance, in agreement with the results found in this work. On the other hand, de Mello et al. [3] attributed the increase in compression energy for their

Table 1
Density and mechanical properties (compression tests) of reinforced foams.

		Density (kg/m^3)	Compression modulus (kPa)	Compressive strength (kPa)	Densification strain (%)
Neat PU	Up	77.4 ± 1.3	62.67 ± 10.88	2.68 ± 0.28	58.55 ± 2.17
	Down	93.0 ± 4.9	91.20 ± 4.20	4.33 ± 0.18	55.62 ± 3.38
1% RHA	Up	77.4 ± 2.7	54.50 ± 2.51	2.66 ± 0.15	61.82 ± 1.56
	Down	86.9 ± 1.9	109.20 ± 2.43	4.77 ± 0.19	57.02 ± 2.53
2% RHA	Up	65.4 ± 9.5	55.85 ± 14.08	2.39 ± 0.26	62.60 ± 1.27
	Down	72.3 ± 4.4	76.51 ± 11.31	3.57 ± 0.31	61.76 ± 2.82
3% RHA	Up	53.0 ± 5.5	34.87 ± 2.98	2.34 ± 0.24	61.69 ± 2.32
	Down	71.4 ± 2.7	60.50 ± 3.36	3.44 ± 0.24	62.21 ± 1.44
5% RHA	Up	56.2 ± 5.2	40.79 ± 2.72	1.96 ± 0.14	63.33 ± 2.67
	Down	66.3 ± 8.3	59.61 ± 7.65	2.74 ± 0.22	61.20 ± 1.37

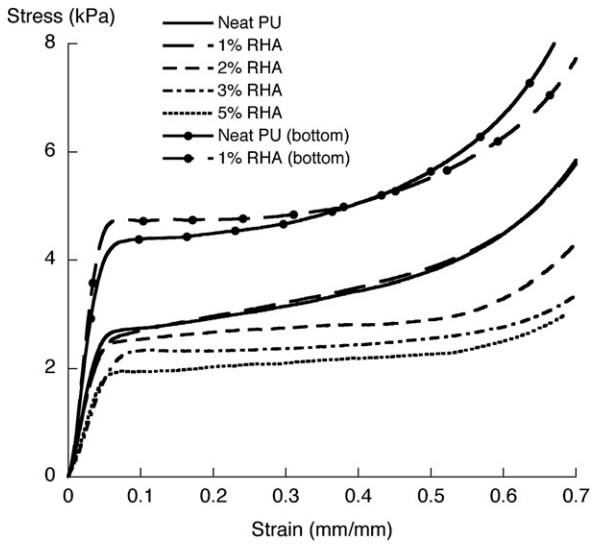

Fig. 2. Compression stress-strain curves for RHA filled and unfilled polyurethane foams.

filled foams to the small size of the PET particles, in addition to the good adhesion between the filler and the PU matrix.

The compression modulus, compressive strength and densification strain of RHA filled foams are also presented in Table 1. In all cases, the compression modulus and compressive strength increase with density, since in compression the stiffness arises from buckling of cell walls [8,22]. The higher density is related to more compact cellular structures, hence there is more material per unit area and the modulus and strength increase [26]. In Fig. 3, the compressive strengths (σ_c) of all samples were plotted as a function of density (δ). The continuous line is evidence

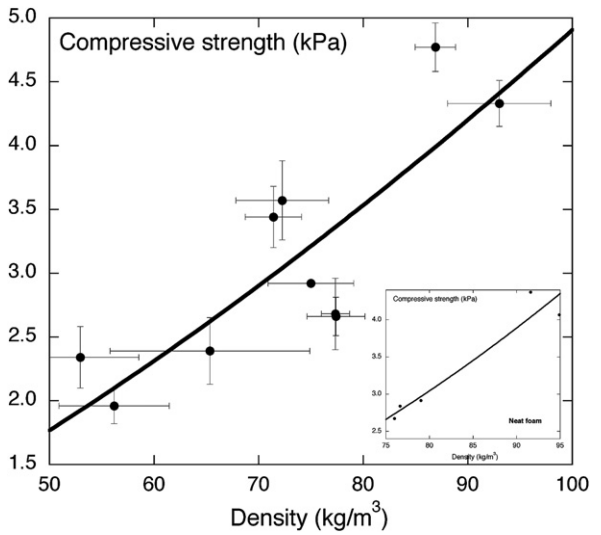

Fig. 3. Compressive strength of RHA filled and unfilled polyurethane foams as a function of density (δ). Inset: compressive strength of neat polyurethane foams vs. δ.

that the relationship σ_c proportional to δ^a [22,27,28] holds in our system. The exponent a is associated with the structure and deformation mechanics of the cellular material. According to Sanders and Gibson [27], the theoretical values of a are 1.5, 2 and 1.36 if the foams are based on open-cells, closed-cells or hollow spheres, respectively. In our case, the best fitting of all data (unreinforced and rice husk filled foams) gives a value of $a = 1.47$, which is very near that of open-celled foam. However, if only the unfilled foam is considered, the fitted value increases up to 2.08 (see inset of Fig. 3), confirming that the open-cells are a consequence of the addition of RHA and not due to the use of the modified tung oil.

On the other hand, the general trend for compressive modulus and compressive strength is to decrease with filler concentration. Samples filled with 1 wt.% RHA and taken from the bottom of the foams are the ones that showed a different tendency, which can be attributed to heterogeneities in these specific foams. This behavior has been reported previously for other filled foams: Guan and Hanna [26] reported that foams had higher mechanical properties when cells were uniform in size, evenly distributed, hexagonal/pentagonal in shape, and unbroken. Verdejo et al. [29] confirmed that the negative impact of the addition of carbon nanotubes (CNTs) on the foam compressive mechanical properties was due to the changes in foam microstructure (i.e. varying densities and cellular structures), which dominate over the reinforcing effect of the CNTs at the very low loading fractions involved in their work (up to 0.2 wt.%). In our case, it was also shown (microscopy analysis) that RHA incorporation causes severe disruption of the foam morphology which results in reduced compression properties.

The overall trend for the densification strain is to increase slightly with RHA content but to decrease with foam density. There are a few exceptions in the most concentrated samples, but they are attributed to specimen heterogeneities. Even the differences between samples are low, this indicates that filled foams can sustain higher deformations without collapsing because they are a little more flexible than the neat polyurethane foams, which can be related to a lower cross-link density. This will be further discussed in the following section (dynamic-mechanical behavior).

Recovery ratio relates to resilience, and refers to the ability of a material to recover its original shape after it has been deformed. A greater recovery ratio indicates a greater degree of rebound of a material after being compressed. Since the foams based on tung oil were rather flexible, R_r was evaluated and is presented in Table 2. It decreases as the density of the foams increase and increases as rice husk ash content increases, especially for the most concentrated samples. However, it is clear that the foams are not perfectly elastic bodies (i.e. complete recovery of the original dimensions when the compression force is released [4]), since the recovery ratio is quite far from 100%. Moreover, the elastic stiffness decrease after a loading/unloading cycle is particularly significant in all cases, as can be seen from the comparison of compression modulus obtained from the first and second compression tests (Tables 1 and 2), indicating that they behave as viscoelastic (VE)

Table 2
Mechanical properties of reinforced foams (compression tests) determined after 1 min of recovery.

		R_r (%)	Compression modulus (2nd test) (kPa)	Compression modulus ratio (2nd/1st)
Neat PU	Up	58.95 ± 0.71	4.87 ± 0.90	0.078
	Down	50.64 ± 2.63	8.42 ± 1.09	0.092
1% RHA	Up	58.92 ± 1.47	5.13 ± 0.34	0.094
	Down	53.88 ± 1.03	7.91 ± 0.56	0.072
2% RHA	Up	65.32 ± 5.07	3.34 ± 0.95	0.060
	Down	61.65 ± 2.36	4.88 ± 0.23	0.064
3% RHA	Up	71.89 ± 2.97	3.08 ± 0.26	0.088
	Down	62.09 ± 1.43	4.20 ± 0.92	0.069
5% RHA	Up	70.18 ± 2.80	3.04 ± 0.40	0.075
	Down	65.38 ± 4.57	4.27 ± 0.53	0.072

(low resilience) foams. In fact, it was indicated that VE foam is prepared using a polyol blend of high- and low-molecular weight polyols and a polymeric isocyanate, including polymeric MDI [30], which are the reagents used in this work.

The dynamic mechanical behavior of composite foams as a function of the temperature is shown in Fig. 4a and b. Data presented in Fig. 4a are useful to confirm the compression behavior, since a decrease in the storage modulus as filler concentration increases is seen. There were, however, some curves that did not strictly follow this trend: the 1% reinforced foam exhibited a larger storage modulus than neat PU foam in the low temperature range (below 65 °C), and the composite containing 2 wt.% RHA presented the lowest storage modulus, although these inconsistencies were attributed to heterogeneities in the selected samples. It should be keep in mind that, by applying both a fixed deformation and a temperature ramp, the transitions and also the defects appear with higher intensities than in static mechanical tests or differential scanning calorimetry (DSC). Moreover, the dynamic mechanical behavior of this polyurethane foam and its derived composites is quite complex, due to both the heterogeneity of the precursors selected to produce the samples (i.e. a high functionalized natural polyol with a wide distribution of molecular weights, polymeric MDI, ethylene glycol, etc.) and to processing problems (high viscosity mixture, particle agglomeration, density variation with foam height).

From Fig. 4a, it is also seen that the glassy to rubbery transition covered a considerable temperature range in all cases, and started at lower temperature as the filler concentration increases. This fact can be more clearly observed from Fig. 4b, where it is also seen that there were at least two wide transitions that appear with quite different intensities in the 0–40 °C and 50–130 °C ranges for the unreinforced and 1 wt.% RHA reinforced foams. The wide ranges of temperatures covered by the transitions indicate that many different relaxation mechanisms are involved. This result is in very good agreement with the comments of Petrovic [31] and our previous results [32]: the broad glass transition observed in these types of cross-linked polymers is the result of the complexity of the vegetable oils derived networks. In fact, the natural polyol obtained from tung oil is a broad mixture of different polyalcohols containing one or two hydroxylated fatty acid chains, as well as small amounts

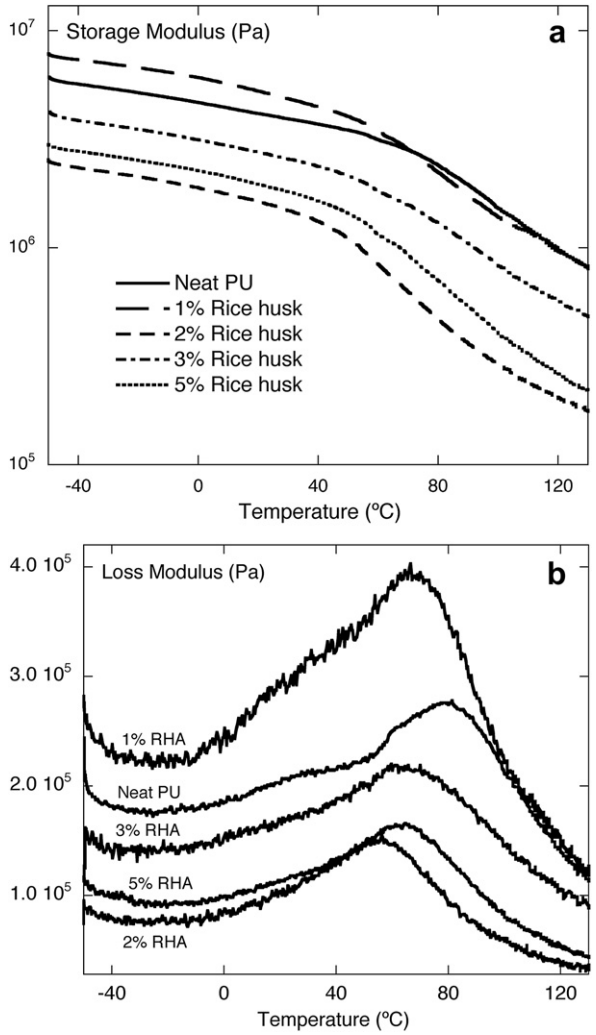

Fig. 4. a) Storage modulus and b) loss modulus as a function of the temperature for RHA filled and unfilled polyurethane foams.

of unreacted agents (triethanolamine) that could not be separated from the final liquid product [32]. Therefore, the glass transitions of network sections with low, medium and high cross-link density become superimposed to achieve the wide transition observed by dynamic-mechanical testing. Moreover, the short diol added in this work to the foam formulation increases the inherent complexity of the system, leading to two broad transition peaks, clearly noticed in formulations containing very low amounts of RHA (0 and 1 wt.%). As Tg values in this temperature range were not previously observed for the compact (not foamed) polyurethanes prepared without the addition of ethylene glycol and cured under pressure and at higher temperature (75 °C as opposed to room temperature) [8,32,33], it is attributed to the relaxation of the pendant chains and low cross-linked zones of the polymeric matrix. For more concentrated samples, this low temperature peak is hardly noticed, probably due to physical interactions developed between the filler and the pendant chains of the polymeric network, which restrict the motion of the latter. On the other

hand, the main transition (which occurs at higher temperature) appears for the neat foam at approximately the same temperature range as that reported in our previous works [8,32,33] and decreases noticeably as filler content increases. Hence, it is related to the relaxation of zones of higher cross-link density, but also to the decreasing level of physical filler-matrix interactions developed in the system, as the result of the increased viscosity of the reactive liquid mixture due to increasing additions of ash. In fact, chemical filler-matrix interactions are not expected in this system, since the rice husk ash contains about 94 wt.% of SiO_2 (without residual char), as confirmed by X-ray fluorescence tests [13]. Regarding these proposed physical filler-matrix interactions, it is interesting to highlight that the larger the concentration of RHA, the lower is the high temperature thermal transition, indicating that the presence of filler increases the chain mobility of the high cross-linked zones of the polymeric matrix, which is associated with a larger fraction of free volume in the network due to lower interaction between the polymer chains. Probably, the presence of particles leads to decreased cross-link density of the polymeric matrix, due to diffusion problems in the high viscosity reactive liquid mixture (i.e. particles interact with liquid reactives, retarding or preventing the formation of urethane bonds). A similar effect was noticed by Silva et al. [16] in one of their works, although the explanation proposed by the group was completely different: they observed that the fibers (cellulose residue, in this case) could induce a decrease in the reactivity of the components of their rigid polyurethane foams since the OH groups of cellulose chemically reacted with part of the MDI, leaving less isocyanate groups available for the reaction with the polyol component.

4. Conclusions

New composite foams with a high percentage of their composition based on renewable resources (polyol derived from tung oil, rice husk ash) were prepared. The replacement of a small part of the modified tung oil by a low molecular weight diol lead to reactive liquid mixtures of adequate viscosity, but also to foams with viscoelastic (low resilience) behavior, that are able to recover part of the deformation applied in compressive tests. Both unreinforced and RHA filled samples exhibited a density gradient in the foam rise direction due to the free rise method selected for the preparation. The addition of rice husk ash led to samples with reduced compression modulus, compressive strength, thermal transitions and storage modulus respect to the unfilled foam, mainly due to detrimental changes induced by the filler on the liquid mixture reactivity and the foam cellular structure. However, densification strain exhibits the opposite behavior indicating that reinforced foams can sustain slightly higher deformations without collapsing.

Acknowledgements

The authors thank CAPES Foundation, Ministry of Education of Brazil, for the fellowship awarded to Lic. V.R. da Silva. M.A. Mosiewicki and N.E. Marcovich thank the financial support of the National Research Council of Argentina (CONICET, Grant PIP 0648) and National University of Mar del Plata (UNMdP, Grant 15/G312 – ING318/11).

References

[1] Z.H. Tu, V.P.W. Shim, C.T. Lim, Plastic deformation modes in rigid polyurethane foam under static loading, International Journal of Solids and Structures 38 (2001) 9267–9279.
[2] M.V. Alonso, M.L. Auad, S.R. Nutt, Modeling the compressive properties of glass fiber reinforced epoxy foam using the analysis of variance approach, Composite Science and Technology 66 (2006) 2126–2134.
[3] D. de Mello, S.H. Pezzin, S.C. Amico, The effect of post-consumer PET particles on the performance of flexible polyurethane foams, Polymer Testing 28 (2009) 702–708.
[4] Q. Fang, M.A. Hanna, Preparation and characterization of biodegradable copolyester–starch based foams, Bioresource Technology 78 (2001) 115–122.
[5] S. Tan, T. Abraham, D. Ference, C.W. Macosko, Rigid polyurethane foams from a soybean oil-based polyol, Polymer 52 (2011) 2840–2846.
[6] R. Gu, M.M. Sain, S.K. Konar, A feasibility study of polyurethane composite foam with added hardwood pulp, Industrial Crops and Products 42 (2013) 273–279.
[7] K.-Y. Lee, L.L.C. Wong, J.J. Blaker, J.M. Hodgkinson, A. Bismarck, Biobased macroporous polymer nanocomposites made by mechanical frothing of acrylated epoxidised soybean oil, Green Chemistry 13 (2011) 3117–3123.
[8] M.A. Mosiewicki, G.A. Dell'Arciprete, M.I. Aranguren, N.E. Marcovich, Polyurethane foams obtained from castor oil-based polyol and filled with wood flour, Journal of Composite Materials 43 (2009) 3057–3072.
[9] H.J. Wang, M.Z. Rong, M.Q. Zhang, J. Hu, H.W. Chen, T. Czigány, Biodegradable foam plastics based on castor oil, Biomacromolecules 9 (2007) 615–623.
[10] M. Carme Coll Ferrer, D. Babb, A.J. Ryan, Characterisation of polyurethane networks based on vegetable derived polyol, Polymer 49 (2008) 3279–3287.
[11] S.P. Wu, J.F. Qiu, M.Z. Rong, M.Q. Zhang, L.Y. Zhang, Plant oil-based biofoam composites with balanced performance, Polymer International 58 (2009) 403–411.
[12] U. Casado, N.E. Marcovich, M.I. Aranguren, M.A. Mosiewicki, High-strength composites based on tung oil polyurethane and wood flour: effect of the filler concentration on the mechanical properties, Polymer Engineering & Science 49 (2009) 713–721.
[13] V.R. Silva, M.A. Mosiewicki, M.I. Yoshida, M.C. Silva, P.M. Stefani, N.E. Marcovich, Polyurethane foams based on modified tung oil and reinforced with rice husk ash I: synthesis and physical chemical characterization, Polymer Testing 32 (2) (2013) 438–445.
[14] P.M. Stefani, V. Cyras, A. Tejeira Barchi, A. Vazquez, Mechanical properties and thermal stability of rice husk ash filled epoxy foams, Journal of Applied Polymer Science 99 (2006) 2957–2965.
[15] G. Tondi, V. Fierro, A. Pizzi, A. Celzard, Tannin-based carbon foams, Carbon 47 (2009) 1480–1492.
[16] M.C. Silva, J.A. Takahashi, D. Chaussy, M.N. Belgacem, G.G. Silva, Composites of rigid polyurethane foam and cellulose fiber residue, Journal of Applied Polymer Science 117 (2010) 3665–3672.
[17] Y. Fujimoto, S.S. Ray, M. Okamoto, A. Ogami, K. Yamada, K. Ueda, Well-controlled biodegradable nanocomposite foams: from microcellular to nanocellular, Macromolecular Rapid Communications 24 (2003) 457–461.
[18] S.Y. Lee, H. Chen, M.A. Hanna, Preparation and characterization of tapioca starch–poly(lactic acid) nanocomposite foams by melt intercalation based on clay type, Industrial Crops and Products 28 (2008) 95–106.
[19] L. Madaleno, R. Pyrz, A. Crosky, L.R. Jensen, J.C.M. Rauhe, V. Dolomanova, A.M.M.V. de Barros Timmons, J.J. Cruz Pinto, J. Norman, Processing and characterization of polyurethane nanocomposite foam reinforced with montmorillonite–carbon nanotube hybrids, Composites Part A: Applied Science and Manufacturing 44 (2013) 1–7.
[20] B. Del Saz-Orozco, M. Oliet, M.V. Alonso, E. Rojo, F. Rodríguez, Formulation optimization of unreinforced and lignin nanoparticle-reinforced phenolic foams using an analysis of variance approach, Composite Science and Technology 72 (2012) 667–674.
[21] P.M. Stefani, A.T. Barchi, J. Sabugal, A. Vazquez, Characterization of epoxy foams, Journal of Applied Polymer Science 90 (2003) 2992–2996.
[22] L.J. Gibson, M.F. Ashby, Cellular Solids: Structure and Properties, Cambridge University Press, Cambridge, 1997.

[23] M.F. Ashby, The properties of foams and lattices, Philosophical Transactions of the Royal Society A: Mathematical, Physical and Engineering Sciences 364 (2006) 15–30.
[24] B. Yin, Z.-M. Li, H. Quan, M.-B. Yang, Q.-M. Zhou, C.-R. Tian, J.-H. Wang, Morphology and mechanical properties of nylon-1010-filled rigid polyurethane foams, Journal of Elastomers and Plastics 36 (2004) 333–349.
[25] I. Javni, W. Zhang, V. Karajkov, Z.S. Petrovic, V. Divjakovic, Effect of nano-and micro-silica fillers on polyurethane foam properties, Journal of Cellular Plastics 38 (2002) 229–239.
[26] J. Guan, M.A. Hanna, Functional properties of extruded foam composites of starch acetate and corn cob fiber, Industrial Crops and Products 19 (2004) 255–269.
[27] W.S. Sanders, L.J. Gibson, Mechanics of hollow sphere foams, Materials Science and Engineering: A 347 (2003) 70–85.
[28] W. Zhao, V. Fierro, A. Pizzi, G. Du, A. Celzard, Effect of composition and processing parameters on the characteristics of tannin-based rigid foams. Part II: physical properties, Materials Chemistry and Physics 123 (2010) 210–217.
[29] R. Verdejo, R. Stämpfli, M. Alvarez-Lainez, S. Mourad, M.A. Rodriguez-Perez, P.A. Brühwiler, M. Shaffer, Enhanced acoustic damping in flexible polyurethane foams filled with carbon nanotubes, Composite Science and Technology 69 (2009) 1564–1569.
[30] K. Ashida, Polyurethane and Related Foams. Chemistry and Technology, CRC Press, Boca Raton, 2007.
[31] Z.S. Petrovic, Polyurethanes from vegetable oils, Polymer Reviews 48 (2008) 109–155.
[32] M.A. Mosiewicki, U. Casado, N.E. Marcovich, M.I. Aranguren, Moisture dependence of the properties of composites made from tung oil based polyurethane and wood flour, Journal of Polymer Research 19 (2012).
[33] M.A. Mosiewicki, U. Casado, N.E. Marcovich, M.I. Aranguren, Polyurethanes from tung oil: polymer characterization and composites, Polymer Engineering & Science 49 (2009) 685–692.